Research Paper

Senescence-like phenotype in post-mitotic cells of mice entering middle age

Marco Raffaele[1,*], Kristina Kovacovicova[1,*], Francesca Bonomini[2,3], Rita Rezzani[2,3], Jan Frohlich[1], Manlio Vinciguerra[1,4]

[1]International Clinical Research Center (FNUSA-ICRC), St' Anne University Hospital, Brno, Czech Republic
[2]Anatomy and Physiopathology Division, Department of Clinical and Experimental Sciences, University of Brescia, Brescia, Italy
[3]Interdepartmental University Center of Research "Adaption and Regeneration of Tissues and Organs-(ARTO)", University of Brescia, Brescia, Italy
[4]Department of Histology and Embryology, Faculty of Medicine, Masaryk University, Brno, Czech Republic
*Equal contribution

Correspondence to: Manlio Vinciguerra; **email:** manlio.vinciguerra@fnusa.cz, manliovinciguerra@gmail.com
Keywords: senescence, mice, markers
Received: April 6, 2020 **Accepted:** May 28, 2020 **Published:** July 7, 2020

ABSTRACT

Staining mice tissues for β-galactosidase activity is a fundamental tool to detect age- or disease-associated cellular senescence. However, reported analyses of positivity for senescence-associated β-galactosidase activity or for other markers of senescence in post-mitotic cells of healthy murine tissues have been fragmentary or inconclusive. Here, we attempted to independently deepen this knowledge using multiple senescence markers within the same cells of wild type mice entering middle age (9 months of age). A histochemistry protocol for the pH-dependent detection of β-galactosidase activity in several tissues was used. At pH 6, routinely utilized to detect senescence-associated β-galactosidase activity, only specific cellular populations in the mouse body (including Purkinje cells and choroid plexus in the central nervous system) were detected as strongly positive for β-galactosidase activity. These post-mitotic cells were also positive for other established markers of senescence (p16, p21 and DPP4), detected by immunofluorescence, confirming a potential senescent phenotype. These data might contribute to understanding the functional relation between the senescence-associated β-galactosidase activity and senescence markers in post-mitotic cells in absence of disease or advanced aging.

INTRODUCTION

Cellular senescence is a cell state implicated in various physiological processes and also in many age-related diseases [1], described for the first time by Hayflick in 1961 [2]. In 2019, the International Cell Senescence Association (ICSA) released a consensus paper on the definition of what constitutes senescent cells: cell senescence is regarded as a state triggered by stress or certain physiological processes, characterized by a stable cell-cycle arrest with secretory features, macromolecular damage, and altered energy metabolism [1]. Conversely, many criteria that define senescent cells have also been observed in a wide range of post-mitotic cells, suggesting that senescence as a stress response can occur in non-dividing cells temporally uncoupled from cell cycle arrest [3, 4]. Rapid gain of interest in cellular senescence is rising from the possibility of therapeutically targeting it to improve healthy aging and age-related disease, using among others drugs called senolytics [5, 6], and from the creation a systematic and comprehensive approach

to the classification and staging of organismal senescence in order to guide aging science policy and gerontology practice [7].

There is currently no single marker with absolute specificity for senescent cells. Some markers have more universal validity while others are related to specific senescent cell types. ICSA advised multi-marker approach, which combines broad and more specific markers for robust detection of senescent cells in tissues. One of the most frequently used marker of cell senescence is the activity of senescence-associated beta-galactosidase (SA-β-gal), hydrolase enzyme that catalyzes the hydrolysis of β-galactosides into monosaccharides [8]. pH is a classic and fundamental factor to discriminate SA-β-gal – operating at pH 6, from bacterial β-Gal – operating at pH 7.4, and from the endogenous β-gal - operating at pH 3–5 [9, 10]. More specific markers include nuclear proteins (*i.e.*, p16, p21) and senescence-associated heterochromatin foci (SAHF), which are specialized domains of facultative heterochromatin that contribute to silencing of proliferation-promoting genes in senescent cells [1, 11, 12]. Moreover, senescent cells are characterized by a secretory associated secretory phenotype (SASP, which includes various interleukins, chemokines, growth factors, inflammatory molecules, ligands and insoluble factors), which can help to confirm the senescent phenotype [1]. SA-β-gal was the first marker allowing the identification of senescent cells in culture and mammalian tissues, and connecting senescence with aging [13, 14]. Since 1995, the wide use of SA-β-gal to study senescence in human or mice tissues *in situ* has been accompanied by controversies and technical challenges. It has been proposed that SA-β-Gal staining does not depend on age but on the presence of certain pathologies and on the proliferative status of the cells studied, appearing even in "young" cells as long as they are not proliferative [15–17].

In this respect, while senescent features have been found to be activated in a range of post-mitotic cells, independent multi-marker integration and confirmation of these results is still lacking for most of them [3, 4].

RESULTS

Here, we performed an analysis for SA-β-gal (pH 6.0) staining on a range of tissues of healthy mice entering middle age (9 months old): heart muscle, skeletal muscle, bone-femur, brain-cortex, brain-hippocampus, brain-cerebellum, choroid plexus, lymph nodes, intestine, pancreas, kidney, visceral adipose tissue, liver and lungs; according to a well-established protocol [18, 19]. The majority of tissues analyzed exhibited cellular populations with strong diffuse β-gal positivity at low pH values (4 to 5), which fainted or disappeared at pH 6 to 7, indicating a non SA-β-gal activity: examples of tissues following this pattern included the hippocampus and the testes (Figures 1 and 2). Conversely, we report strong SA-β-gal staining (pH 6) in cerebellum (Figure 3), choroid plexus (Figure 4), pancreatic islets (Figure 5) and basal/stem cells in the intestinal crypts (Figure 6) of adult wild type mice. A distinct β-galactosidase staining was detected from pH 4 to SA-β-gal-associated pH 6 specifically for the Purkinje cell layer, containing the large GABAergic neurons constituting the output of all motor coordination in the cerebellar cortex, and not for small granule neurons (Figure 3). Obesity or high fat diet results in the accumulation of senescent cells in the mouse brain [1, 20]. We found a SA-β-gal staining pattern in the cerebellum of 9 weeks old adult leptin receptor deficient *ob/ob* mice that was identical to the one observed in

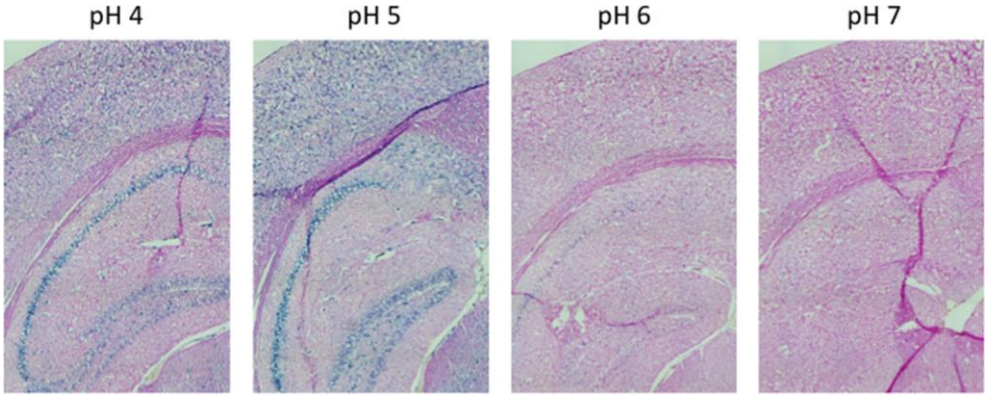

Figure 1. pH-dependent (pH 4 to pH 7) β-gal activity in frozen sections of 9 months old C57/Bl6J mice hippocampus. Nuclear Fast Red was used for counterstaining. At pH 6, specific for SA-β-gal, no marked β-gal activity is evident. Representative images from 3 different mice are shown.

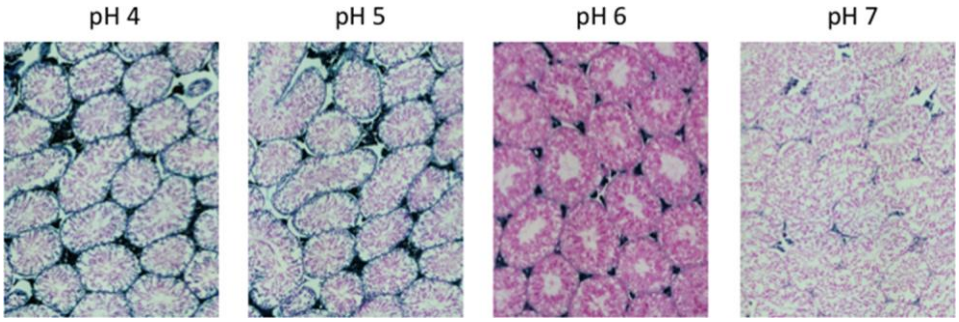

Figure 2. pH-dependent (pH 4 to pH 7) β-gal activity in frozen sections of 9 months old C57/Bl6J mice testes. Nuclear Fast Red was used for counterstaining. At pH 6, specific for SA-β-gal, no marked β-gal activity is evident. Representative images from 3 different mice are shown.

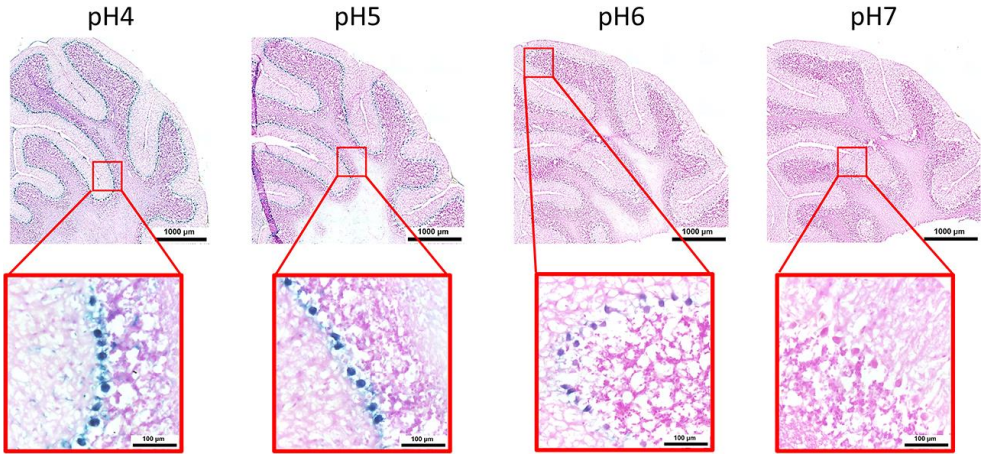

Figure 3. pH-dependent (pH 4 to pH 7) β-gal activity in frozen sections of mouse cerebellum. 9 months old C57/Bl6J. Nuclear Fast Red was used for counterstaining. At pH 6, specific for SA-β-gal, bluish color from β-gal activity is evident specifically in the Purkinje cell layer. Representative images from 3 different mice are shown.

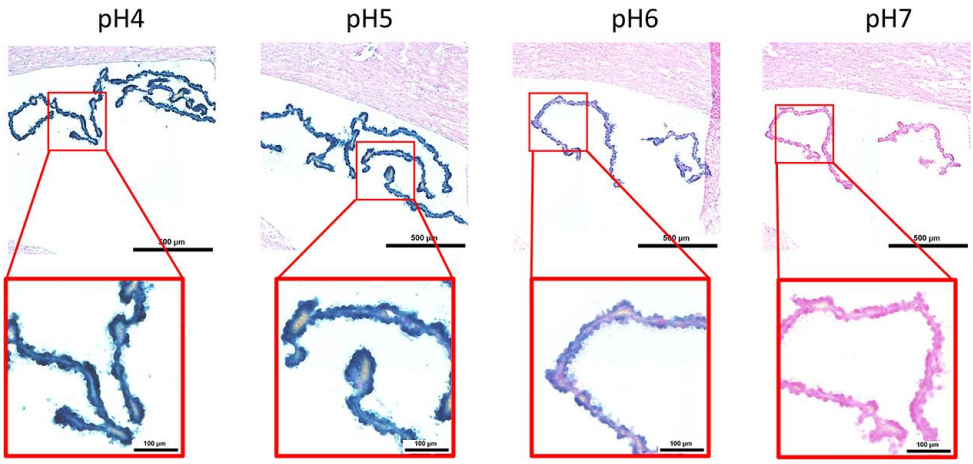

Figure 4. pH-dependent (pH 4 to pH 7) β-gal activity in frozen sections of mouse choroid plexus. 9 months old C57/Bl6J. Nuclear Fast Red was used for counterstaining. At pH 6, specific for SA-β-gal, bluish color from β-gal activity is evident specifically in ependymal cells in the choroid plexus. Representative images from 3 different mice are shown.

wild type mice (Supplementary Figure 1), thus obesity-independent. Next, we tested the positivity of Purkinje cell layer for β-gal and for other established positive (p16, p21 and DPP4 [19, 21–24]) and negative (H3K4me3 [25]) markers of cell senescence by immunofluorescence staining in wild type mice, as recommended recently to verify a senescent phenotype [1]. Surprisingly, in the cerebellum, Purkinje cells were strongly immunopositive for p16, p21 and DPP4 expression, while they were negative for H3K4me3 that instead stained intensely small granule neurons (Figure 7). Within the central nervous system (CNS) of wild type mice, we detected a distinct β-gal staining at pH 4 and SA-β-gal staining at pH 6 specifically in the choroid plexus, which produces the cerebrospinal fluid in the ventricles of the brain and consists of modified ependymal cells (Figure 4). The observed β-galactosidase staining pattern was identical in the choroid plexus of *ob/ob* mice (Supplementary Figure 2). Ependymal cells were found strongly immunopositive for p16, p21 and DPP4 expression, while staining for H3K4me3 was present but irregular and patchy compared to the other markers (Figure 8). Altogether, our findings demonstrate *a bona fide* senescent-like phenotype of adult mouse cell types/tissues (Purkjnie cell layer, choroid plexus, pancreatic islets and intestinal crypts), based on SA-β-gal staining and other markers of senescence.

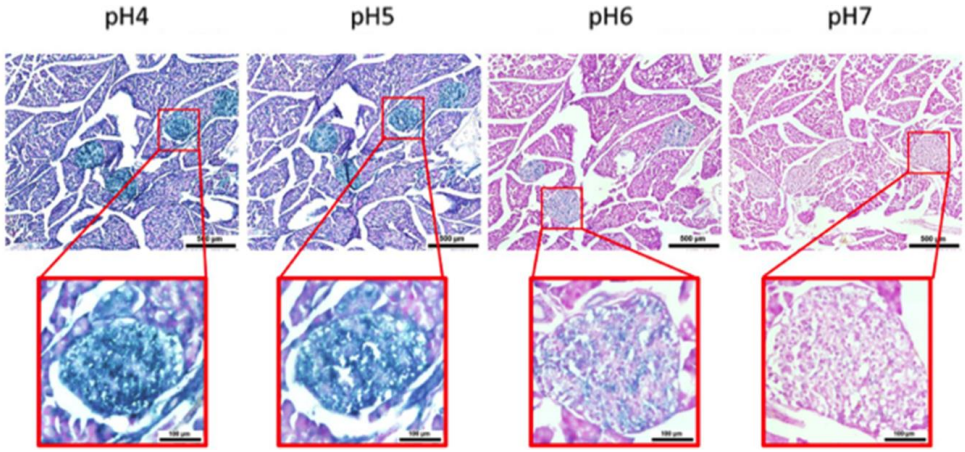

Figure 5. pH-dependent (pH 4 to pH 7) β-gal activity in frozen sections of 9 months old C57/Bl6J mouse pancreas. Nuclear Fast Red was used for counterstaining. At pH 6, specific for SA-β-gal, bluish color from β-gal activity is evident specifically in pancreatic islets. Representative images from 3 different mice are shown.

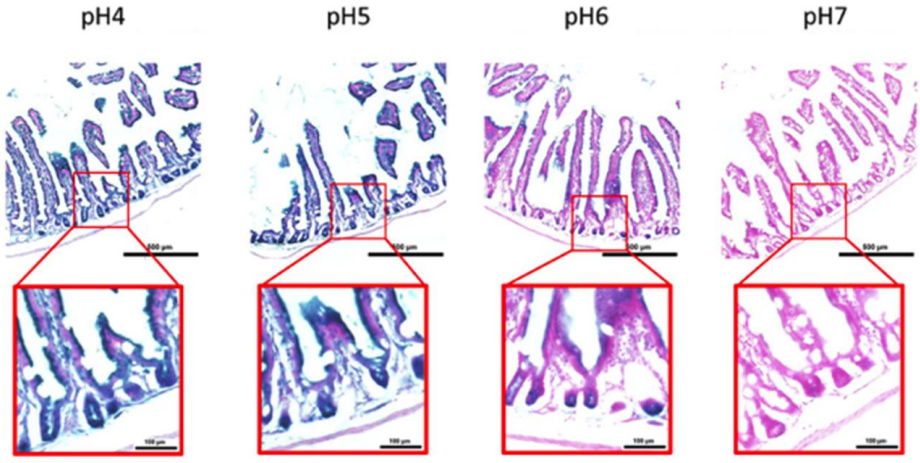

Figure 6. pH-dependent (pH 4 to pH 7) β-gal activity in frozen sections of 9 months old C57/Bl6J mouse intestine. Nuclear Fast Red was used for counterstaining. At pH 6, specific for SA- β-gal, bluish color from β-gal activity is evident specifically in cells located basally in the intestinal crypts. Representative images from 3 different mice are shown.

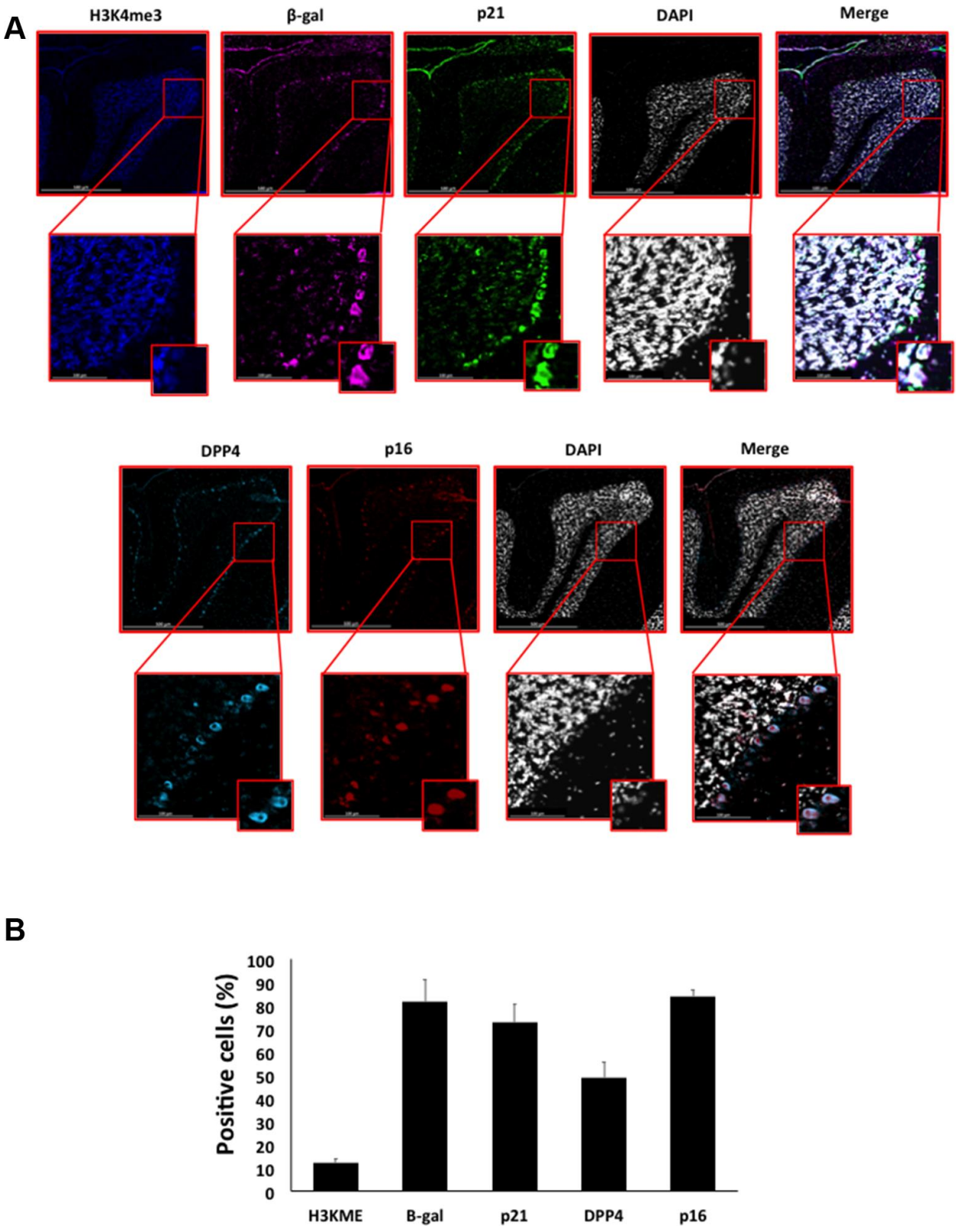

Figure 7. (**A**) Immunofluorescent staining of senescence markers in Purkinje cells of 9 months old C57/Bl6J mouse cerebellar cortex. Images display H3K4me3 (blue), β-gal (purple), p21 (green), DPP4 (cyan) p16 (red) and DAPI-stained nuclei (white) fluorescence signals. The corresponding multichannel overlaid images are shown in the right column. All these markers, except H3K4me3, show an increased localization and expression in Purkinje cells. Representative images from 3 different mice are shown. (**B**) Frequency of positive cells for each marker as in (**A**), indicated in %.

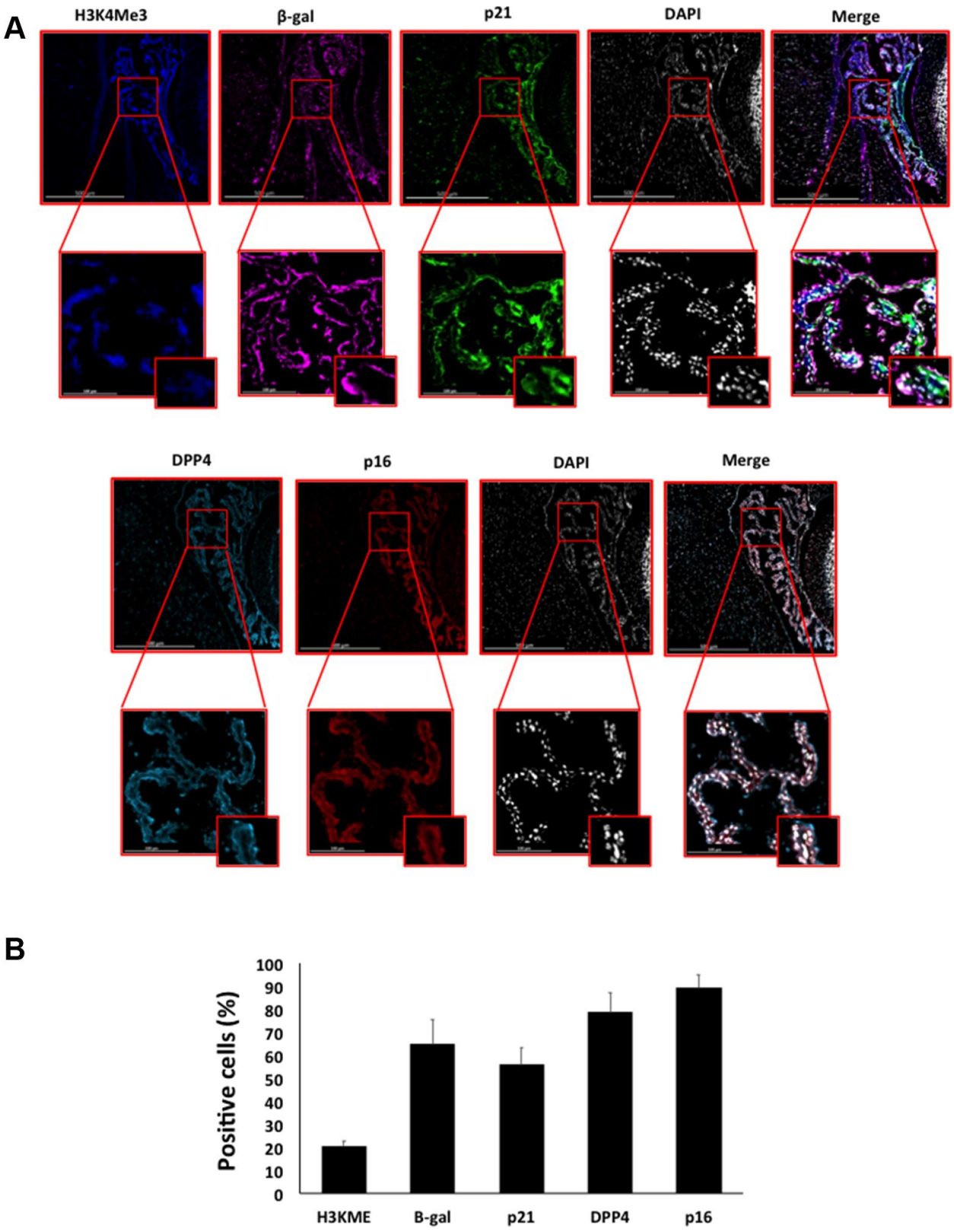

Figure 8. (**A**) Immunofluorescent staining of senescence markers of 9 months old C57/Bl6J mouse choroid plexus. Images display H3K4me3 (blue), β-gal (purple), p21 (green), DPP4 (cyan) p16 (red) and DAPI-stained nuclei (white) fluorescence signals. The corresponding multichannel overlaid images are shown in the right column. All these markers show an increased localization and expression in choroid plexus cells. Representative images from 3 different mice are shown. (**B**) Frequency of positive cells for each marker as in (**A**), indicated in %.

DISCUSSION

Endogenous β-galactosidase staining (pH 4) has been described in murine pancreatic islets [10]. To our knowledge ours is the first study reporting SA-β-gal in pancreatic islets: cells residing in the islets of Langerhans are terminally differentiated cells and almost entirely in a post-mitotic state [26]. Positive SA-β-gal staining in intestinal crypts is in agreement with previous findings showing increasing γH2AX foci-positive crypt enterocytes in old mice [27–29]; in this respect, SA-β-gal positive cells within the intestinal crypts could be Paneth cells, which are entirely post-mitotic cells [30]. Future studies of colocalization of SA-β-gal staining and Paneth cells specific markers (i.e lysozyme) will shed light on this issue.

Post-mitotic cells are essential for the function of the brain. Recently, it was shown that Purkinje cells from old (32 months of age), but not from young (4 months of age), displayed oxidative stress, γH2AX and SA-β-gal staining: a co-localization of multiple senescence markers in the same neurons [31]. This was the first study describing a "senescence-like phenotype" in post-mitotic cells of old, but not young, healthy mice. Our data are fully consistent and demonstrate that the senescence-like phenotype of Purkinje cell layer might actually start before middle age in mice, as middle age in mice is considered to start around 10 months of age [32]. Low bacterial β-gal staining was previously detected in the choroid plexus in mice [33, 34]. Our data on SA-β-gal stained choroid plexus are reminiscent of those showing increased expression of markers of senescence, particularly those related to obesity-induced inflammation, in the periventricular area adjacent to the lateral ventricle, which is located near the root of the choroid plexus [20]. Choroid plexus produces CSF and participate in brain immunosurveillance. During ageing, CSF secretion decreases as much as 50%. These modifications are concurrent with subnormal brain activity, reduced beta-amyloid clearance, and increased glycation phenomena as well as oxidative stress [35]. The potential interplay between senescent phenotype of the choroid plexus at young/mid age and its functional decline at older age is unknown. Senescence markers have been observed in neurons in the CNS also in a pathological context, during ischemia or Alzheimer's disease [36, 37].

Accumulation of multiple senescence markers in aging mice has been shown for major post-mitotic cells types residing in different tissues, such as retinal ganglion cells, cardiomyocytes, skeletal myofibers, cochlear cells and osteocytes (reviewed in [3]) The physiological or aging role of the potential senescent phenotype – as we identified by SA-β-gal, p16, p21 and DPP4 marker expression levels - in the different functions performed by Purkinje cells and ependymal cells, specialized post-mitotic neuronal cell types positive, in not aged healthy mice remains unclear. During rat post-natal cerebella development, the period of maximal differentiation between days 9 to 13 was associated with a change in p21 and p16 staining from the external granular and Purkinje cells to a primarily Purkinje cell distribution [38]. Expression levels of H3K4me3 and DPP4 and their signaling pathways have been implicated in several aspects of murine brain homeostasis, from development to aging [39–42]. To our knowledge, ours is the first report to detect expression of DPP4 in Purkinje cells; DPP4 inhibitors are new promising therapeutic approach against Alzheimer's disease [41]. Future research on senescent post-mitotic cells should encompass also the crucial role of mammalian target of rapamycin (mTOR) pathway. During cell cycle arrest caused by contact inhibition cells do not undergo a fully senescent phenotype. It was demonstrated that the conversion from cell cycle arrest to senescence, a phenomenon called geroconversion, requires stimulation of mTOR and downstream effectors, such as pS6K, concomitantly to p16/p21 activation [43, 44]. Therefore, our study thus encourages exploring the function of post-mitotic cells positive for SA-β-gal activity and other senescence markers in healthy adult or middle age organisms, by simultaneous assessment of related phenomena (including SASP, the last step of the proposed multi-marker, three-step workflow for detecting senescent cells [1]), to understand whether post-mitotic senescence plays a significant role as driver of ageing phenotypes.

MATERIALS AND METHODS

Mice

The C57BL/6 mice strains were purchased from AnLab, Czech Republic. All animal work was conducted in accordance with Act No 246/1992 Coll., on the protection of animals against cruelty under the supervision of the Central Commission for Animal Welfare, approval 39197/2018-MZE-17214. Mice were housed under controlled conditions (light-dark cycle 12 h, 21 ± 2 °C, 40–50% humidity) with food and water available ad libitum. Obese (*ob/ob*) male mice in BL6 background (Charles River, MA, US) were housed in the University of Brescia animal facility (Brescia, Italy). Mice of 9-weeks-of-age were then euthanized and organs were removed. The experimental protocol n°516/2018-PR granted was approved by the University of Brescia Institutional Animal Care Committee (Brescia, Italy) and was conducted in accordance with national and European regulations. After mice sacrifice all tissues were collected, washed in PBS, fixed in 4%

paraformaldehyde for 24h and de-hydrate in sucrose 5% at least for 24hr. Finally, they were embedded in OCT and sectioned in 10μM slices with a frozen microtome.

Histochemistry

B-galactosidase detection method was performed as previously described [18, 19]. Briefly, tissues sections were fixed in 1% formalin in PBS for 1 min at RT, washed three times in PBS and incubated overnight on X-gal staining solution [1 mg/mL of X-gal (VWR), 40 mM citric acid/sodium phosphate buffer, 5 mM potassium ferricyanide (Sigma), 5 mM potassium ferrocyanide (Sigma), 150 mM NaCl, and 2 mM MgCl2] at 37°C in a humidified chamber. The experiments were carried out using staining solutions at different pH (from 4 to 7) to assess the SA-β-gal activity. Samples were rinsed with distilled water and counterstained with Nuclear Fast Red (Sigma) for 5 minutes. Images were acquired using Pia-Apochromat 20x 0.8 M27objective on Axio scan Z1 (Zeiss).

Immunofluorescence

Immunofluorescence staining was performed on mice tissues sections as previously described [45–48]. Mice tissues sections were re-hydrate in PBS for 10 min and treated with the TrueBlack Autofluorescence quencher (Biotium) for 30 sec. After careful washing in PBS, sections were blocked for 60 min in M.O.M blocking solution (Vector Laboratories) and then incubated with primary antibody overnight. Two primary antibodies co-staining solutions were used on adjacent sections to detect target proteins: one mix containing p21 (ab80633), B-gal (ab9361) and H3K4me3 (ab213224); and another mix containing CDKN2A/p16INK4a (ab189034) and anti-DPPIV/CD26 (R&D Systems MAB1180). All the antibodies were used at 1:500 dilution except for anti-DPPIV/CD26 that was used at 1:1000. The staining was developed using Alexa fluorescent (488, 555, 647) conjugated secondary antibodies, and images were acquired using Axio scan Z1 (Zeiss).

Data analysis

Image analysis was performed using ImageJ (http://rsb.info.nih.gov/ij/), ZEN 2011 SP1 (black edition) version 8.1., or ZEN 2 version 2.0.0.0. (Carl Zeiss Microscopy GmbH).

Positivity for each marker was decided if the cellular signal intensity was clearly above background intensity seen in the isotype negative controls. Greater than 80 Purkinje cells and > 200 choroid plexus cells were counted per animal and stained marker. Data were presented as means ± SD of 3 animals for group.

CONFLICTS OF INTEREST

The authors declare no conflicts of interest.

FUNDING

This work was supported by a grant from the European Social Fund and European Regional Development Fund - Project MAGNET (No. CZ.02.1.01/0.0/0.0/15_003/0000492) (to M.V.).

REFERENCES

1. Gorgoulis V, Adams PD, Alimonti A, Bennett DC, Bischof O, Bishop C, Campisi J, Collado M, Evangelou K, Ferbeyre G, Gil J, Hara E, Krizhanovsky V, et al. Cellular senescence: defining a path forward. Cell. 2019; 179:813–27. https://doi.org/10.1016/j.cell.2019.10.005 PMID:31675495

2. Hayflick L, Moorhead PS. The serial cultivation of human diploid cell strains. Exp Cell Res. 1961; 25:585–621. https://doi.org/10.1016/0014-4827(61)90192-6 PMID:13905658

3. von Zglinicki T, Wan T, Miwa S. Senescence in post-mitotic cells: a driver of aging? Antioxid Redox Signal. 2020. [Epub ahead of print]. https://doi.org/10.1089/ars.2020.8048 PMID:32164429

4. Sapieha P, Mallette FA. Cellular senescence in postmitotic cells: beyond growth arrest. Trends Cell Biol. 2018; 28:595–607. https://doi.org/10.1016/j.tcb.2018.03.003 PMID:29704982

5. Wissler Gerdes EO, Zhu Y, Tchkonia T, Kirkland JL. Discovery, development, and future application of senolytics: theories and predictions. FEBS J. 2020; 287:2418–27. https://doi.org/10.1111/febs.15264 PMID:32112672

6. Longo VD, Antebi A, Bartke A, Barzilai N, Brown-Borg HM, Caruso C, Curiel TJ, de Cabo R, Franceschi C, Gems D, Ingram DK, Johnson TE, Kennedy BK, et al. Interventions to slow aging in humans: are we ready? Aging Cell. 2015; 14:497–510. https://doi.org/10.1111/acel.12338 PMID:25902704

7. Calimport SR, Bentley BL, Stewart CE, Pawelec G, Scuteri A, Vinciguerra M, Slack C, Chen D, Harries LW, Marchant G, Fleming GA, Conboy M, Antebi A, et al. To help aging populations, classify organismal senescence. Science. 2019; 366:576–78.

https://doi.org/10.1126/science.aay7319
PMID:31672885

8. Rouwenhorst RJ, Pronk JT, van Dijken JP. The discovery of beta-galactosidase. Trends Biochem Sci. 1989; 14:416–18.
https://doi.org/10.1016/0968-0004(89)90292-2
PMID:2510375

9. Merkwitz C, Blaschuk O, Schulz A, Ricken AM. Comments on methods to suppress endogenous β-galactosidase activity in mouse tissues expressing the LacZ reporter gene. J Histochem Cytochem. 2016; 64:579–86.
https://doi.org/10.1369/0022155416665337
PMID:27555495

10. Inada A, Nienaber C, Bonner-Weir S. Endogenous beta-galactosidase expression in murine pancreatic islets. Diabetologia. 2006; 49:1120–22.
https://doi.org/10.1007/s00125-006-0186-7
PMID:16541278

11. Aird KM, Zhang R. Detection of senescence-associated heterochromatin foci (SAHF). Methods Mol Biol. 2013; 965:185–96.
https://doi.org/10.1007/978-1-62703-239-1_12
PMID:23296659

12. Lo Re O, Vinciguerra M. Histone MacroH2A1: a chromatin point of intersection between fasting, senescence and cellular regeneration. Genes (Basel). 2017; 8:367.
https://doi.org/10.3390/genes8120367 PMID:29206173

13. Dimri GP, Lee X, Basile G, Acosta M, Scott G, Roskelley C, Medrano EE, Linskens M, Rubelj I, Pereira-Smith O. A biomarker that identifies senescent human cells in culture and in aging skin in vivo. Proc Natl Acad Sci USA. 1995; 92:9363–67.
https://doi.org/10.1073/pnas.92.20.9363
PMID:7568133

14. Lee BY, Han JA, Im JS, Morrone A, Johung K, Goodwin EC, Kleijer WJ, DiMaio D, Hwang ES. Senescence-associated beta-galactosidase is lysosomal beta-galactosidase. Aging Cell. 2006; 5:187–95.
https://doi.org/10.1111/j.1474-9726.2006.00199.x
PMID:16626397

15. Cristofalo VJ. SA beta gal staining: biomarker or delusion. Exp Gerontol. 2005; 40:836–38.
https://doi.org/10.1016/j.exger.2005.08.005
PMID:16181758

16. Yegorov YE, Akimov SS, Hass R, Zelenin AV, Prudovsky IA. Endogenous beta-galactosidase activity in continuously nonproliferating cells. Exp Cell Res. 1998; 243:207–11.
https://doi.org/10.1006/excr.1998.4169
PMID:9716464

17. Severino J, Allen RG, Balin S, Balin A, Cristofalo VJ. Is beta-galactosidase staining a marker of senescence in vitro and in vivo? Exp Cell Res. 2000; 257:162–71.
https://doi.org/10.1006/excr.2000.4875
PMID:10854064

18. Itahana K, Campisi J, Dimri GP. Methods to detect biomarkers of cellular senescence: the senescence-associated beta-galactosidase assay. Methods Mol Biol. 2007; 371:21–31.
https://doi.org/10.1007/978-1-59745-361-5_3
PMID:17634571

19. Kovacovicova K, Vinciguerra M. Isolation of senescent cells by iodixanol (OptiPrep) density gradient-based separation. Cell Prolif. 2019; 52:e12674.
https://doi.org/10.1111/cpr.12674
PMID:31517418

20. Ogrodnik M, Zhu Y, Langhi LG, Tchkonia T, Krüger P, Fielder E, Victorelli S, Ruswhandi RA, Giorgadze N, Pirtskhalava T, Podgorni O, Enikolopov G, Johnson KO, et al. Obesity-induced cellular senescence drives anxiety and impairs neurogenesis. Cell Metab. 2019; 29:1061–77.e8.
https://doi.org/10.1016/j.cmet.2018.12.008
PMID:30612898

21. Kovacovicova K, Skolnaja M, Heinmaa M, Mistrik M, Pata P, Pata I, Bartek J, Vinciguerra M. Senolytic cocktail Dasatinib+Quercetin (D+Q) does not enhance the efficacy of senescence-inducing chemotherapy in liver cancer. Front Oncol. 2018; 8:459.
https://doi.org/10.3389/fonc.2018.00459
PMID:30425964

22. Matjusaitis M, Chin G, Sarnoski EA, Stolzing A. Biomarkers to identify and isolate senescent cells. Ageing Res Rev. 2016; 29:1–12.
https://doi.org/10.1016/j.arr.2016.05.003
PMID:27212009

23. Kim KM, Noh JH, Bodogai M, Martindale JL, Yang X, Indig FE, Basu SK, Ohnuma K, Morimoto C, Johnson PF, Biragyn A, Abdelmohsen K, Gorospe M. Identification of senescent cell surface targetable protein DPP4. Genes Dev. 2017; 31:1529–34.
https://doi.org/10.1101/gad.302570.117
PMID:28877934

24. Idda ML, McClusky WG, Lodde V, Munk R, Abdelmohsen K, Rossi M, Gorospe M. Survey of senescent cell markers with age in human tissues. Aging (Albany NY). 2020; 12:4052–66.
https://doi.org/10.18632/aging.102903
PMID:32160592

25. Chicas A, Kapoor A, Wang X, Aksoy O, Evertts AG, Zhang MQ, Garcia BA, Bernstein E, Lowe SW. H3K4 demethylation by Jarid1a and Jarid1b contributes to

retinoblastoma-mediated gene silencing during cellular senescence. Proc Natl Acad Sci USA. 2012; 109:8971–76. https://doi.org/10.1073/pnas.1119836109 PMID:22615382

26. Klochendler A, Caspi I, Corem N, Moran M, Friedlich O, Elgavish S, Nevo Y, Helman A, Glaser B, Eden A, Itzkovitz S, Dor Y. The genetic program of pancreatic β-cell replication in vivo. Diabetes. 2016; 65:2081–93. https://doi.org/10.2337/db16-0003 PMID:26993067

27. Wang C, Jurk D, Maddick M, Nelson G, Martin-Ruiz C, von Zglinicki T. DNA damage response and cellular senescence in tissues of aging mice. Aging Cell. 2009; 8:311–23. https://doi.org/10.1111/j.1474-9726.2009.00481.x PMID:19627270

28. Wang C, Maddick M, Miwa S, Jurk D, Czapiewski R, Saretzki G, Langie SA, Godschalk RW, Cameron K, von Zglinicki T. Adult-onset, short-term dietary restriction reduces cell senescence in mice. Aging (Albany NY). 2010; 2:555–66. https://doi.org/10.18632/aging.100196 PMID:20844316

29. Jurk D, Wilson C, Passos JF, Oakley F, Correia-Melo C, Greaves L, Saretzki G, Fox C, Lawless C, Anderson R, Hewitt G, Pender SL, Fullard N, et al. Chronic inflammation induces telomere dysfunction and accelerates ageing in mice. Nat Commun. 2014; 2:4172. https://doi.org/10.1038/ncomms5172 PMID:24960204

30. Clevers H. The intestinal crypt, a prototype stem cell compartment. Cell. 2013; 154:274–84. https://doi.org/10.1016/j.cell.2013.07.004 PMID:23870119

31. Jurk D, Wang C, Miwa S, Maddick M, Korolchuk V, Tsolou A, Gonos ES, Thrasivoulou C, Saffrey MJ, Cameron K, von Zglinicki T. Postmitotic neurons develop a p21-dependent senescence-like phenotype driven by a DNA damage response. Aging Cell. 2012; 11:996–1004. https://doi.org/10.1111/j.1474-9726.2012.00870.x PMID:22882466

32. Flurkey K Currer JM, Harrison DE. Chapter 20 - Mouse Models in Aging Research. In: The Mouse in Biomedical Research (Second Edition), Volume III, Pages 637-672. American College of Laboratory Animal Medicine (Elsevier); 2007. https://doi.org/10.1016/B978-012369454-6/50074-1

33. Devlin LA, Ramsbottom SA, Overman LM, Lisgo SN, Clowry G, Molinari E, Powell L, Miles CG, Sayer JA. Embryonic and foetal expression patterns of the ciliopathy gene CEP164. PLoS One. 2020; 15:e0221914. https://doi.org/10.1371/journal.pone.0221914 PMID:31990917

34. Bolon B. Whole mount enzyme histochemistry as a rapid screen at necropsy for expression of beta-galactosidase (LacZ)-bearing transgenes: considerations for separating specific LacZ activity from nonspecific (endogenous) galactosidase activity. Toxicol Pathol. 2008; 36:265–76. https://doi.org/10.1177/0192623307312693 PMID:18369090

35. Serot JM, Béné MC, Faure GC. Choroid plexus, aging of the brain, and Alzheimer's disease. Front Biosci. 2003; 8:s515–21. https://doi.org/10.2741/1085 PMID:12700093

36. Musi N, Valentine JM, Sickora KR, Baeuerle E, Thompson CS, Shen Q, Orr ME. Tau protein aggregation is associated with cellular senescence in the brain. Aging Cell. 2018; 17:e12840. https://doi.org/10.1111/acel.12840 PMID:30126037

37. Oubaha M, Miloudi K, Dejda A, Guber V, Mawambo G, Germain MA, Bourdel G, Popovic N, Rezende FA, Kaufman RJ, Mallette FA, Sapieha P. Senescence-associated secretory phenotype contributes to pathological angiogenesis in retinopathy. Sci Transl Med. 2016; 8:362ra144. https://doi.org/10.1126/scitranslmed.aaf9440 PMID:27797960

38. Watanabe G, Pena P, Shambaugh GE 3rd, Haines GK 3rd, Pestell RG. Regulation of cyclin dependent kinase inhibitor proteins during neonatal cerebella development. Brain Res Dev Brain Res. 1998; 108:77–87. https://doi.org/10.1016/s0165-3806(98)00032-7 PMID:9693786

39. Barral S, Beltramo R, Salio C, Aimar P, Lossi L, Merighi A. Phosphorylation of histone H2AX in the mouse brain from development to senescence. Int J Mol Sci. 2014; 15:1554–73. https://doi.org/10.3390/ijms15011554 PMID:24451138

40. Park S, Kim GW, Kwon SH, Lee JS. Broad domains of histone H3 lysine 4 trimethylation in transcriptional regulation and disease. FEBS J. 2020. [Epub ahead of print]. https://doi.org/10.1111/febs.15219 PMID:31967712

41. Angelopoulou E, Piperi C. DPP-4 inhibitors: a promising therapeutic approach against Alzheimer's disease. Ann Transl Med. 2018; 6:255. https://doi.org/10.21037/atm.2018.04.41

PMID:30069457

42. Baker DJ, Petersen RC. Cellular senescence in brain aging and neurodegenerative diseases: evidence and perspectives. J Clin Invest. 2018; 128:1208–16. https://doi.org/10.1172/JCI95145 PMID:29457783

43. Leontieva OV, Demidenko ZN, Blagosklonny MV. Contact inhibition and high cell density deactivate the mammalian target of rapamycin pathway, thus suppressing the senescence program. Proc Natl Acad Sci USA. 2014; 111:8832–37. https://doi.org/10.1073/pnas.1405723111 PMID:24889617

44. Blagosklonny MV. Rapamycin, proliferation and geroconversion to senescence. Cell Cycle. 2018; 17:2655–65. https://doi.org/10.1080/15384101.2018.1554781 PMID:30541374

45. Bolasco G, Calogero R, Carrara M, Banchaabouchi MA, Bilbao D, Mazzoccoli G, Vinciguerra M. Cardioprotective mIGF-1/SIRT1 signaling induces hypertension, leukocytosis and fear response in mice. Aging (Albany NY). 2012; 4:402–16. https://doi.org/10.18632/aging.100464 PMID:22691943

46. Pazienza V, Panebianco C, Rappa F, Memoli D, Borghesan M, Cannito S, Oji A, Mazza G, Tamburrino D, Fusai G, Barone R, Bolasco G, Villarroya F, et al. Histone macroH2A1.2 promotes metabolic health and leanness by inhibiting adipogenesis. Epigenetics Chromatin. 2016; 9:45. https://doi.org/10.1186/s13072-016-0098-9 PMID:27800025

47. Lo Re O, Fusilli C, Rappa F, Van Haele M, Douet J, Pindjakova J, Rocha SW, Pata I, Valčíková B, Uldrijan S, Yeung RS, Peixoto CA, Roskams T, et al. Induction of cancer cell stemness by depletion of macrohistone H2A1 in hepatocellular carcinoma. Hepatology. 2018; 67:636–50. https://doi.org/10.1002/hep.29519 PMID:28913935

48. Lo Re O, Mazza T, Giallongo S, Sanna P, Rappa F, Vinh Luong T, Li Volti G, Drovakova A, Roskams T, Van Haele M, Tsochatzis E, Vinciguerra M. Loss of histone macroH2A1 in hepatocellular carcinoma cells promotes paracrine-mediated chemoresistance and $CD4^+/CD25^+/FoxP3^+$ regulatory T cells activation. Theranostics. 2020; 10:910–24. https://doi.org/10.7150/thno.35045 PMID:31903159

SUPPLEMENTARY MATERIALS

Supplementary Figures

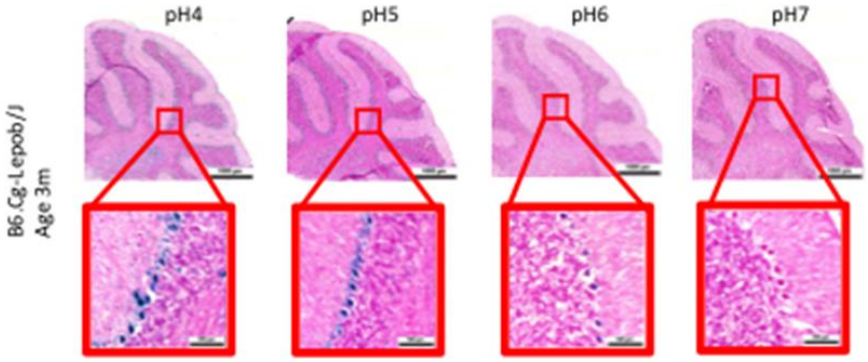

Supplementary Figure 1. pH-dependent (pH 4 to pH 7) β-gal activity in frozen sections of mouse cerebellum from 3 month old leptin receptor-deficient *ob/ob* mice. Nuclear Fast Red was used for counterstaining. At pH 6, specific for SA-β-gal, bluish color from β-gal activity is evident specifically in the Purkinje cell layer. Representative images from 3 different mice per genotype are shown.

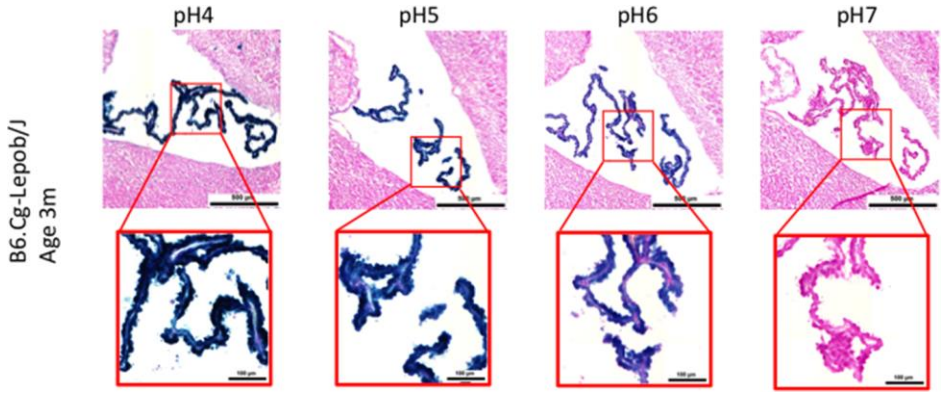

Supplementary Figure 2. pH-dependent (pH 4 to pH 7) β-gal activity in frozen sections of choroid plexus from 3 months old leptin receptor-deficient *ob/ob* mice. Nuclear Fast Red was used for counterstaining. At pH 6, specific for SA-β-gal, bluish color from β-gal activity is evident specifically in ependymal cells in the choroid plexus. Representative images from 3 different mice are shown.